Neuronal hemoglobin induces α-synuclein cleavage and loss of dopaminergic neurons

Santulli Chiara[1*], Bon Carlotta[2*], De Cecco Elena[1], Codrich Marta[1], Narkiewicz Joanna[1] Parisse Pietro[3], Perissinotto Fabio[3], Claudio Santoro[4], Francesca Persichetti[4], Legname Giuseppe[1], Stefano Espinoza[2,4#] and Gustincich Stefano[1,2#]

1. Area of Neuroscience, Scuola Internazionale Superiore di Studi Avanzati (SISSA), Trieste, Italy.
2. Central RNA Laboratory, Istituto Italiano di Tecnologia (IIT), Genova, Italy.
3. ELETTRA Synchrotron Light Source, Trieste, Italy.
4. Department of Health Sciences and Research Center on Autoimmune and Allergic Diseases (CAAD), University of Piemonte Orientale (UPO), Novara, Italy.

* equally contributed to the paper

#Corresponding author:
Stefano Gustincich
Deputy Director for Life Sciences
Director – Central RNA Laboratory
Istituto Italiano di Tecnologia (IIT)
via Melen 83, Genova (GE) 16152 - Italy
Tel: +39-010-71781-447
e-mail: stefano.gustincich@iit.it

Correspondence may also be addressed to:
Stefano Espinoza
Central RNA Laboratory
Istituto Italiano di Tecnologia (IIT)
via Melen 83, Genova (GE) 16152 – Italy
e-mail: stefano.espinoza@iit.it

ABSTRACT

Backgroud

α-synuclein, a protein involved in the pathogenesis of several neurodegenerative disorders, is subjected to several post-translational modifications. Among them, C-terminal truncation seems to increase its aggregation propensity *in vitro*. Hemoglobin is the major protein in erythrocytes to carries oxygen and recently is found to be expressed in dopaminergic neurons and to be involved in the pathogenesis of neurodegenerative diseases such as Parkinson's disease.

Methods

To assess the role of hemoglobin in α-synuclein post-translational modification and in dopamine cells physiology, we over-expressed α and β-chains of Hb in iMN9D dopamine cells to evaluate its effect on α-synuclein truncation. Using an AAV9 we expressed α and β-chains of hemoglobin in dopamine neurons of Substantia Nigra pars compacta and evaluate its effect on α-synuclein post-translational modification, dopamine neurons survivals and behavioural outcome.

Results

The over-expression of α and β-chains of hemoglobin in iMN9D dopamine cells increased C-terminal truncation of α-synuclein when cells were treated with α-synuclein preformed fibrils. This cleavage was led at least in part by Calpain protease. Hemoglobin over-expression in Substantia Nigra pars compacta induced a similar pattern of α-synuclein truncation and a decrease in tyrosine hydroxylase expression, unveiling a decrease of dopamine neurons of about 50%. This dopamine cells loss led to a mild motor impairment and a deficit in recognition and spatial working memory.

Conclusion

Our study reveals a novel role for hemoglobin in α-synuclein post-translational modification and in dopamine neurons homeostasis suggesting neuronal hemoglobin is an important modifier in synucleinopathies such as Parkinson's disease.

KEYWORDS

α-synuclein; synucleinopathies; hemoglobin; Parkinson's disease.

BACKGROUND

α-synuclein (α-syn) is a 140-amino acid protein predominantly located at pre-synaptic terminals in association with synaptic vesicles. The regulatory role of α-syn in vesicle trafficking (1) is believed to be its main physiological function. However, it is also implicated in synaptic maintenance and SNARE protein assembly (2, 3).

α-syn can undergoes misfolding as monomers may tend to assume a pathologic β-sheet conformation, leading to the formation of amyloid assemblies, also known as amyloid seeds (4). The spreading within and between neuronal and glial cells occurs via a prion-like recruitment of endogenous protein into further pathologic forms. Indeed, *in vitro and in vivo* models corroborate the prion-like "conformational templating" through the exposure of preformed α-syn fibril seeds to monomers (Ms) that induce fibril elongation triggering aggregation (5-7).

In addition, pathologic α-syn present several post-translational modifications (PTMs) among which, phosphorylation at serine 129 (pSer-129) and truncations are the most abundant within the inclusions (8, 9). *In vitro,* C-terminal truncation potentiate the aggregation propensity of C-terminal truncated species (ΔC-α-syn) into toxic fibrils with an increased prion-like seeding activity as compared with the full-length (FL-α-syn) (4, 6, 10, 11).

Misfolding of this protein and consequent pathological inclusion formation is a hallmark of the class of neurodegenerative diseases termed synucleinopathies (12), which includes Parkinson's Disease (PD), Lewy Body Dementia (LBD) and Multiple System Atrophy (MSA). PD and LBD are pathologically characterized by neuronal Lewy Body (LB) inclusions observed in the intracellular spaces of *Substantia Nigra pars compacta* (SNpc) neurons and composed of amyloidogenic α-syn of which 10—30% of total is C-terminal truncated (13, 14). Instead, MSA is characterised by α-syn-containing glial cytoplasmic inclusions (GCIs) within the oligodendrocytes (15). The formation and the continued presence of α-syn oligomers and fibrils is causative of neuronal and glial toxicity. Along with LB inclusions, PD present selective degeneration of A9 dopaminergic (DA) neurons of SNpc.

Gene expression profiling of A9 DA neurons revealed the expression of hemoglobin (Hb) α and β-chain (16-18). Although the main functions of neuronal Hb (nHb) in the brain remains unclear, there is evidence that it has a role in mitochondrial

homeostasis. nHb has been found to constitute complexes with α-syn ($nHb^{\alpha\text{-syn}}$) in neuronal tissue (19), consistently supported by nHb-forming insoluble aggregates found in the nucleolus of DA neurons as well as in PD post-mortem brains (18). In the SNpc, $nHb^{\alpha\text{-syn}}$ increase in an age-dependent manner in the cytoplasm, reducing the mithocondrial fraction of free nHb (20) and therefore contribute to an imbalance in mitochondrial homeostasis. Hb overexpression alter gene expression modulating transcript levels of genes involved in oxygen homeostasis and oxidative phosphorylation. The resulting oxidative stress induce iron release from heme promoting mitochondrial dysfunction, α-syn aggregation, and neuronal cell death (21-23). Hb overexpression increases the susceptibility to both MPP^+ (1-methyl-4-phenylpyridinium) and rotenone *in vitro*, increasing nucleolar stress and inhibiting autophagy induced by neurochemical insults (17). Overall, this evidence indicates nHb as major player to DA cells' dysfunction in PD.

Here, we show that Hb increases α-syn truncation *in vitro* and *in vivo* and that Hb expression in SNpc induces a loss of DA neurons and motor and cognitive impairments.

MATERIAL AND METHODS

Production of recombinant human α-synuclein

Expression and purification of human α-syn were performed as previously describe (24). Briefly, α-syn gene was cloned in pET-11a vector and expressed in *E.coli* BL21(DE3) strain. Cells were grown in Luria-Bertani medium at 37°C and expression of α-syn was induced by addition of 0.6 mM isopropyl-β-D-thiogalactoside (IPTG) followed by incubation at 37°C for 5 hours. The protein was extracted and purified according to Huang *et al*. (25).

Fibrillation of human α-synuclein

Lyophilized human α-syn was re-suspended in ddH_2O, filtered with a 0,22 µm syringe filter and the concentration was determined by absorbance measured at 280 nm. Fibrillization reactions were carried out in a 96-well plate (Perkin Elmer) in the presence of a glass bead (3 mm diameter, Sigma) in a final reaction volume of 200 µL. Human α-syn (1.5 mg/ml) was incubated in the presence of 100 mM NaCl, 20 mM TrisHCl pH 7.4 and 10 uM thioflavin T (ThT). Plates were sealed and incubated in

BMG FLUOstar Omega plat reader at 37°C with cycles of 50 seconds shaking (400 rpm) and 10 seconds rest. Formation of fibrils was monitored by measuring the fluorescence of ThT (excitation: 450 nm, emission: 480 nm) every 15 minutes. After reaching the plateau phase, the reactions were stopped. Fibrils were collected, centrifuged at 100000g for 1 hour, resuspended in sterile PBS and stored at -80°C for further use. For cell culture experiments, the fibrillation reaction was carried out without ThT and PFFs in 0,5 ml conical plastic tubes were sonicated for 5 minutes in a Branson 2510 Ultrasonic Cleaner prior addition to cell culture medium.

Cleaning procedures

For fibrils inactivation, all contaminated surfaces and laboratory wares, both reusable and disposable, were cleaned using a 1 % SDS solution prior washing with Milli-Q water according to Bousset *et al.* (26).

Atomic Force Microscopy

Atomic Force Microscopy (AFM) was performed as previously described (27). Briefly, three to five µl of fibril solution was deposited onto a freshly cleaved mica surface and left to adhere for 30 minutes. Samples were then washed with distilled water and blow-dried under a flow of nitrogen. Images were collected at a line scan rate of 0.5-2 Hz in ambient conditions. The AFM free oscillation amplitudes ranged from 25 nm to 40 nm, with characteristic set points ranging from 75% to 90% of these free oscillation amplitudes.

Cell line

MN9D-Nurr1$^{Tet\text{-}on}$ (iMN9D) cell line stably transfected with pBUD-IRES-eGFP (CTRL cells) or with pBUD-β-globin-MYC IRES-eGFP, 2xFLAG-α-globin (Hb cells) were used (16). Cells were maintained in culture at 37 °C in a humidified CO_2 incubator with DMEM/F12 medium (Gibco by Life Technologies, DMEM GlutaMAX® Supplement Cat. No. 31966-021; F-12 Nutrient Mix GlutaMAX® Supplement Cat. No. 31765-027) supplemented with 10% fetal bovine serum (Euroclone, Cat. No. ECS0180L), 100 µg/ml penicillin (Sigma–Aldrich), 100 µg/ml streptomycin (Sigma-Aldrich). 300 µg/ml neomycin (Gibco by Life Technologies, Cat. No 11811-031) and 150 µg/ml zeocyn (Invivogen, Cat. No. ant-zn-05) were used for selection.

Exposure of iMN9D cells to α-syn monomers and fibrils

iMN9D cells were exposed to 2 µM of α-syn species (2 µM equivalent monomer concentration in the case of amyloids) in cell culture media for 24, 48, 96 hours before collection.

For western blot analysis cells were plated in 6 well-plate ($6x10^5$ cells/plate for 24h collection, $3x10^5$ cells/plate for 48h collection, $2x10^5$ cells/plate for 96h collection). Additionally, at 96 hours cells were split and maintained for three additional days before collection as Passage 1 (P1). Cells treated with vehicle were used as control (Untreated).

For immunocytochemistry, cells were cultured in 12-well plates with coverslips ($3x10^5$ cells/well for 24h collection, $1,5x10^5$ cells/well for 48h collection, $1x10^5$ cells/well for 96h collection).

For MTT analysis, cells were cultured in 96-well plates ($4x10^4$ cells/well for 24h collection, $2x10^4$ cells/well for 48h collection, $1x10^4$ cells/well for 96h collection).

MTT analysis

Cell viability was assayed using Thiazolyl Blue Tetrazolium Bromide (MTT, Sigma–Aldrich, M5655) following the manufacturer's instructions. Briefly, 20 µl of MTT solution (5 mg/ml in PBS) were added to each well and incubated at 37°C for 4 h. The medium was then removed and replaced with 200 µl DMSO. Plates were shaken before absorbance measurements. Absorbance was measured at 550 nm wavelength using a microplate ELISA reader (Thermo Scientific).

Western Blot

iMN9D cells were washed 2 times with D-PBS and lysed in 300 µl SDS sample buffer 2X (6 well-plate), briefly sonicated, boiled and 10 µl/sample loaded on 15 % or 8 % (for Spectrin α II immunoblot) SDS-PAGE gel. For antibodies validation, cells were lysed in cold lysis buffer (10 mM Tris-HCl pH 8, 150 mM NaCl, 0.5% Igepal CA-630, 0.5% sodium deoxycholate) supplemented protease inhibitor mixture (Roche Diagnostics, COEDTAF-RO). Lysates were incubated for 30 minutes at 4 °C on rotator and cleared at 12000xg for 20 minutes at 4 °C. Supernatants were transferred in new tubes and total protein content was measured using bicinchoninic acid protein (BCA) quantification kit (Pierce) following the manufacturer's instructions. For SNpc lysates,

dissected brain area was lysed in cold RIPA buffer and centrifuged for 10 minutes at 17,000xg. Sample buffer was added to the supernatant and boiled at 95°C for 5 minutes and 30 µg of proteins were loaded on a 10% SDS-PAGE gel. Proteins were transferred to nitrocellulose membrane (Amersham™, Cat. No. GEH10600001) for 1:30 hour at 100V or 16 hours 20V (only for Spectrin α II immunoblot). Membranes were blocked with 5% non-fat milk or 5% BSA (only for Spectrin α II immunoblot) in TBST solution (TBS and 0.1% Tween20) for 40 minutes at room temperature. Membranes were then incubated with primary antibodies at room temperature for 2 h or overnight at 4 °C (only for Spectrin α II immunoblot). The following antibodies were used: anti-FLAG 1:2000 (Sigma–Aldrich, F3165), anti-MYC 1:2000 (Cell Signaling, 2276), anti-β-actin 1:5000 (Sigma–Aldrich, A5441), anti-Hemoglobin 1:1000 (Cappel, MP Biomedicals, 55039) and anti-GFP 1:1000 (Clontech, 632380), anti-α-syn 1:1000 (C-20) (Santa Cruz Biotechnology, sc-7011-R), anti-α-syn 1:1000 (SYN-1) (BD Transduction Laboratories, 610787), anti-biotin-HRP (Jackson ImmunoResearch Laboratories), anti-Spectrin α II 1:1000 (Santa Cruz, Cat. No. sc-46696), anti-TH 1:1000 (Millipore). For development, membranes were incubated with secondary antibodies conjugated with horseradish peroxidase (Dako) for 1 hour at room temperature. For IP and pulldown experiments, membranes were incubated with Protein A antibody conjugated with horseradish peroxidase for 1 hour at room temperature. Proteins of interest were visualized with the Amersham ECL Detection Reagents (GE Healthcare by SIGMA, Cat. No. RPN2105) or LiteAblot TURBO Extra-Sensitive Chemioluminescent Substrate (EuroClone, Cat. No. EMP012001). Western blotting images were acquired using with Alliance LD2-77WL system (Uvitec, Cambridge) and band intensity was measured UVI-1D software (Uvitec, Cambridge).

Antibodies validation for quantitative western blot

For antibodies validation, cells were lysed in cold lysis buffer (10 mM TrisHCl pH 8, 150 mM NaCl, 0.5% Igepal CA-630, 0.5% sodium deoxycholate) supplemented with protease inhibitor mixture (Roche Diagnostics, COEDTAF-RO). Lysates were incubated for 30 min at 4°C on rotator and cleared at 12000 g for 20 min at 4°C. Supernatants were transferred in new tubes and total protein content was measured using bicinchoninic acid protein (BCA) quantification kit (Pierce) following the

manufacturer's instructions.

Pull-down assay of biotinylated fibrils

For pulldown experiments, α-syn PFFs were biotinylated following the manufacturer's instructions (Sigma-Aldrich). iMN9D cells were lysed in cold immunoprecipitation (IP) buffer (50 mM Tris HCl pH 8, 150 mM NaCl, 0.1% Igepal CA-630) containing protease inhibitors (Roche Diagnostics, COEDTAF-RO). Following 30 min incubation at 4 °C on rotator, lysates were cleared at 12000 g for 20 min and incubated with biotinylated fibrils overnight at 4°C on rotator. Biotinylated fibrils were pulled down by binding to NeutrAvidin Agarose Resin (Pierce, 29200). After 4 h incubation at 4 °C, the resin-bound complexes were washed three times with IP buffer and eluted with SDS sample buffer 2X, boiled at 95°C for 5 min and analysed by western blot.

Cathepsin D and Calpain inhibitors treatment

Pepstatin (Pep, Cathepsin D inhibitor, MedChem Express Cat. No. HY-P0018) and Calpain inhibitor III (Santa Cruz Cat. No. SC-201301) were dissolved in dimethylsulfoxide (DMSO) and diluted in cell culture medium to a final concentration respectively of 100 µM and 10 µM. Hb cells were treated with vehicle (DMSO), Calpain inhibitor III and Pepstatin A at the indicated concentrations for 24 h. Medium was then removed and replaced with new one containing α-syn amyloids, as previously reported, and protease inhibitors to a final concentration respectively of 100 µM and 10 µM, as the day before. Cells were collected at the indicated time points for western blot analysis. Immunoblot of Spectrin α II was used to monitor Calpain inhibitor activity, while Cathepsin D activity kit was uses to monitor Cathepsin D activity.

Cathepsin D activity assay

Cathepsin D (CatD) activity measurements were performed using the Cathepsin D activity assay kit (BioVision, Cat. N. K143) following manufacturer's instructions. Briefly, cells were washed twice with PBS, collected in culture media and pelleted by centrifugation at 500 g for 5 min. Cells were counted and $1x10^5$ cells/well were used. Cells were washed once with PBS, pelleted again by centrifugation at 500 g for 5 min and lysed in CD Cell Lysis Buffer incubating samples for 10 min on ice. Cells were then centrifuged at maximum speed for 10 min. As control, untreated cells were

incubated with PepA (100 µM final concentration) at 37°C for 10 min prior addition of Reaction Buffer and CD substrate (Positive control). The reaction was left to proceed at 37°C for 1:30 h in the dark. Fluorescence was read using Thermo Scientific Varioskan® Flash with a 328-nm excitation filter and 460-nm emission filter. CD activity in relative fluorescence units (RFU) was then normalized to Hb cells treated with vehicle and indicated as % Activity. Each sample was measured in duplicate and measurements were repeated two times.

RNA isolation, Reverse Transcription (RT) and quantitative RT-PCR (qRT-PCR)

Total RNA was extracted using TRIzol Reagent (Thermo Fisher, 15596026) and following manufacturer's instructions. RNA samples were subjected to TURBO DNase (Invitrogen, Cat. No. AM1907) treatment, to avoid DNA contamination. The final quality of RNA sample was tested on 1 % agarose gel with formaldehyde. A total of 1 µg of RNA was subjected to retrotranscription using iScript™cDNA Synthesis Kit (Bio-Rad, Cat. No. 1708890), according to manufacturer's instructions. qRT-PCR was carried out using SYBR green fluorescent dye (iQ SYBR Green Super Mix, Bio-Rad, Cat. No. 1708884) and an iCycler IQ Real time PCR System (Bio-Rad). The reactions were performed on diluted cDNA (1:2). Mouse actin was used as normalizing control in all qRT-PCR experiments. The amplified transcripts were quantified using the comparative Ct method and the differences in gene expression were presented as normalized fold expression with ΔΔCt method [36, 37]. The following primer pairs were used:

β-actin: fwd CACACCCGCCACCAGTTC, rev CCCATTCCCACCATCACACC;
Capn1: fwd TTGACCTGGACAAGTCTGGC, rev CCGAGTAGCGGGTGATTATG;
Capn2: fwd ATGCGGAAAGCACTGGAAG, rev GACCAAACACCGCACAAAAT;
Ctsd: fwd CAGGACACTGTATCGGTTCCA, rev CAAAGACCGGAAGCACGTTG.

Animals

All animal experiments were performed in accordance with European guidelines for animal care and following Italian Board Health permissions (D.Lgs. 26/2014, 4 March 2014). Mice were housed and bred in IIT – Istituto Italiano della Tecnologia (Genova, GE, Italy) animal facility, with 12 hours dark/night cycles and controlled temperature and humidity. Food and water were provided *ad libitum*.

Behavioral testing

All procedures involving animals and their care were carried out in accordance with the guidelines established by the European Community Council (Directive 2010/63/EU of September 22, 2010) and were approved by the Italian Ministry of Health (DL 116/92; DL 111/94-B)

Locomotor activity

To measure spontaneous locomotor activity WT mice injected with AAV9 were placed in the locomotor activity chambers (Omnitech Digiscan, Accuscan Instruments, Columbus, OH, USA) for 60 minutes and total distance travelled was measured by analyzing infrared beam interruptions.

Rotarod

For this test we used a Rotarod from TSE Systems. Briefly, mice are handled on alternate days during the week preceding the start of the Rotarod test (3 handling sessions; 1 min per mouse per session). Behavioral testing lasts two days. On day 1, in the morning, mice are habituated to rotation on the rod under a constant speed of 4 rpm for three trials (60-s inter-trial interval). Trial ends when mice fall off the rod or until they are able to stay on the rod for 300 s. In the afternoon, the test starts by placing the mice on the rod and beginning rotation at constant 4 rpm-speed for 60 seconds. Then the accelerating program is launched for three trials (60-s inter-trial interval) and trial ends when mice fall off the rod or until they are able to stay on the rod for 300 s. Time stayed on the rod was automatically recorded. Mice are tested for two consecutive days (only with the “afternoon program”). The average time spent on the rod is calculated.

Static rods

Five wooden rods of varying thickness (35, 25, 15, 10 and 8 mm diameter) each 60 cm long are fixed to a laboratory shelf such that the rods horizontally protrude into space. The height of the rods above the floor is 60 cm. Mice were placed at the far end of the widest rod, with the orientation of the mouse outward. Two measures are considered: orientation time (time taken to orientate 180° from the starting position towards the shelf) and transit time (the time taken to travel to the shelf end). Orientation

is dependent on the mouse staying upright. If it turns upside down and clings below the rod, it is assigned the maximum orientation score of 120 sec. If, after orienting, the mouse falls or it reaches the maximum test time (arbitrarily set at 120 sec) mice are not tested on smaller rods. After testing on one rod mice are placed back to the home cage to rest while other mice are tested. This procedure is repeated for all the rods. If the mouse fall off the rod within 5 seconds, it is replaced to allow another attempt (as falling within 5 sec could be due to faulty placing by the experimenter), for a maximum of three trials, and the best result is considered. The time for orientation and transit are plotted in the graphs for statistical analysis. Since in smaller rods many of the mice fall or do not complete the test (with the time of 120 sec assignment), the success rate of the test is also calculated as the number of mice that complete the test and the Chi-square test is used to compare the two groups of mice.

Horizontal bars

For this test two bars made of brass are used, 40 cm long, held 50 cm above the bench surface by a wooden support column at each end. Two bar diameters are available: 2 and 4mm. The 2 mm bar is the standard one and more simple for the mice to stay attached on with the forepaw. The larger diameter bar is more difficult since the mice cannot grip those so well. The operator take the mouse by the tail, place it on the bench in front of the apparatus, slide it quickly backwards about 20 cm (this aligns it perpendicular to the bar), rapidly raise it and let it grasp the horizontal bar at the central point with its forepaws only, and release the tail, simultaneously starting the clock. The time to reach one of the end columns of the bar is calculated. The maximum test time (cut-off time) is 30 sec. If the mouse fails to grasp the bar properly first time or fall within 5 sec, the score is not recorded, the mouse is placed back to the cage to rest and then the trial is repeat up to three times since it may be a poor placement of the operator. The best score is taken out of these trials. The score is calculated as an average of the scores of the 2mm and 4 mm bar trials as calculated below:

Falling between 1-5 sec = 1

Falling between 6-10 sec = 2

Falling between 11-20 sec = 3

Falling between 21-30 sec = 4

Falling after 30 sec = 5

The maximum score for completing the test is 5 for each bar and 10 for both bars.

Novel object recognition test

Mice are handled on alternate days during the week preceding the start of the test (3 handling sessions; 1 min per mouse per session on Day 1, 3, 5.). On day 6, mice were subjected to the habituation session in the empty open field for 1 hour. The intensity of the light on the apparatus is of about 60 lux. On day 7, each mouse is subjected to two successive sessions (one acquisition session and one retention trial at 1 hour later). Pre-test session (acquisition trial): each mouse is introduced into the open field containing two identical copies of the same object for 10 minutes. At the end of the session the mouse was returned into the home cage. II session (retention trial): after 1 hour from the acquisition trial, both objects were substituted, one with a third copy of previous object and the other with a new object. This session lasted 5 minutes. The animals are considered to be exploring the object when the head of the animal is facing the object (at a distance < 1 cm) or the animal is touching or sniffing the object. Mice that explored object for <4 sec are excluded. The type of the objects and their positions of presentation during acquisition and retention phase are counterbalanced across animals. A preference index, a ratio of the amount of time spent exploring any one of the objects (training session) or the novel one (retention session) over the total time spent exploring both objects, is used to measure recognition memory. In the pre-test session is counted the total amount of exploration (in sec) for the identical objects and to verify that there is no preference for one of the two side of the chamber where the objects are located.

Y-maze Spontaneous Alternation Test

The apparatus use is a Y-shaped maze with three opaque arms spaced 120° apart with a measure of 40 x 8 x 15cm each. An overhead camera is mounted to ceiling directly above apparatus to monitor mice movement and 4 standing lamps with white light bulbs are placed at corners outside privacy blinds pointed away from apparatus. The arms are labeled as A, B or C to identify the entries. The animal is placed just inside arm B facing away from center and allowed to move through apparatus for 10 minutes while being monitored by automated tracking system. Trial begins

immediately and ends when defined duration has elapsed. Scoring consists of recording each arm entry (defined as all four paws entering arm). The total entries in all arms is recorded. A spontaneous alternation occurs when a mouse enters a different arm of the maze in each of 3 consecutive arm entries. Spontaneous alternation % is then calculated as ((#spontaneous alternation/(total number of arm entries-2))x100.

Stereotaxy AAV9 injection

Adult (12 weeks old) male C57BI/6J mice were used for experiments. Mice were anesthetized by a mixture of Isoflurane/Oxygen and placed on a stereotaxic apparatus (David Kopf instrument, Tujunga, CA, USA) with mouse adaptor and lateral ear bars. The skin on the skull was cut and one hole was made on the same side by a surgical drill. A stereotaxic injection of 1 µl of viral vector suspension (AAV9-CTRL or a mixture of AAV9-2xFLAG-α-globin and AAV9-β-globin-MYC, called AAV9-Hb; titer: – $5*10^{12}$ vg/ml) was delivered bilaterally to SNpc at the following coordinates: anterior/posterior (A/P) −3.2 mm from bregma, medio/lateral (M/L) −1.2 mm from bregma and dorso/ventral (D/V) − 4.5 mm from the dura. The coordinates were calculated according to the Franklin and Paxinnos Stereotaxic Mouse Atlats. Injection rate was 1 µl /15 minutes using a glass gauge needle. After the infusion, the needle was maintained for another 1 minute in the same position and then retracted slowly.

Tissue collection and processing

At 10 months after injection of AAVs into SNpc, the animals were sacrificed. Following induction of deep anaesthesia with an overdose of a mixture of Xylazina and Zoletil, the animals were intensively perfused transcardially with PBS 1 ×. For biochemical analysis, SNpc was dissected and immediately frozen in liquid nitrogen and stored at −80 °C, pending analyses. For immunohistochemical analysis, after the intensively transcardially perfusion with PBS 1X, animals were perfused with 4% paraformaldehyde diluted in PBS 1X. Brains were postfixed in 4% paraformaldehyde for 1 h at 4 °C. The regions containing the SN were cut in 40 µm free-floating slides with a vibratome (Vibratome Series 1000 Sectioning System, Technical Products International, St. Louis, MO, USA). Four consecutive series were collected in order to represent the whole area of interest.

Immunocytochemistry

Cells were washed two times with D-PBS, fixed in 4% paraformaldehyde for 20 minutes, washed two times with PBS 1X and treated with 0.1M glycine for 4 minutes in PBS 1X, washed two times and permeabilized with 0.1% Triton X-100 in PBS 1X for 4 minutes. Cells were then incubated in blocking solution (0.2% BSA, 1% NGS, 0.1% Triton X-100 in PBS 1X), followed by incubation with primary antibodies diluted in blocking solution for 2:30 hours at room temperature. After two washes in PBS 1X, cells were incubated with labelled secondary antibodies and 1µg/ml DAPI (for nuclear staining) for 60 minutes. Cells were washed twice in PBS 1X and once in Milli-Q water and mounted with Vectashield mounting medium (Vector Lab, H-1000). The following antibodies were used: anti-FLAG 1:100 (Sigma–Aldrich, F7425), anti-MYC 1:250 (Cell Signaling, 2276), anti-α-syn (C-20) 1:200 (Santa Cruz Biotechnology, sc-7011-R), anti-α-syn (SYN-1) 1:200 (BD Transduction Laboratories, 610787) and anti-α-syn(phosphoS129) 1:200 (Abcam, ab59264). For detection, Alexa Fluor-488, -594 or -647 (Life Technologies) antibodies were used. Image acquisition was performed using C1 Nikon confocal microscope (60x oil, NA 1.49, 7x zoom-in).

Immunofluorescence with labelled α-syn fibrils

Human α-syn fibrils were fluorescently labelled with Alexa-488 succinimidyl esther (Thermo Fisher Scientific, A20000) following manufacturer's instructions and the unbound fluorophore was removed with multiple dialysis steps in sterile PBS. Uptake experiments were performed following standard IF protocol or following the protocol described by Karpowicz *et al.* [35]. Briefly, cells seeded on coverslips were incubated with culture medium containing labelled α-syn fibrils for 24 h. Prior to standard immunocytochemistry protocol, fluorescence from non-internalized fibrils was quenched by incubating with Trypan Blue for 5 minutes. Cells were then fixed in 4% paraformaldehyde for 20 minutes, washed two times and permeabilized with 0.1% Triton X-100 in PBS 1X for 4 minutes and incubated with HCS Blue Cell Mask 1:1000 for 30 minutes (Thermo Fisher Scientific). Cells were washed twice in PBS 1X and once in Milli-Q water and mounted with Vectashield mounting medium (Vector Lab, H-1000). Images acquisition was performed using C1 Nikon confocal microscope (60x oil, NA 1.49, 7x zoom-in) as z-stacks of 0.5 µm.

Immunohistochemistry

For immunohistochemistry, free-floating slides were rinsed three times in 0.1M phosphate buffered saline (PBS; pH 7.6), contained 0.1% Triton X-100 between each incubation period. All sections were quenched with 3% H_2O_2/10% for 10 min, followed by several changes of buffer. As a blocking step, sections were then incubated in 7% normal goat serum and 0.1% Triton-X 100 for 2 hours at room temperature. This was followed by incubation in primary antibody diluted in 3% normal goat serum and 0.1% Triton-X 100 at 4°C for 24 hrs. The antibody used was an anti-TH diluted 1:500 (AB-152, Millipore). After incubation with the primary antibody, sections were rinsed and then incubated for 2 hours at room temperature with biotinylated secondary antibodies (anti-rabbit 1:1000; Thermo Scientific) in the same buffer solution. The reaction was visualized with avidin-biotin-peroxidase complex (ABC-Elite, Vector Laboratories), using 3,3-diaminobenzidine as a chromogen. Sections were mounted on super-frost ultra plus slides (Thermo Scientific), dehydrated in ascending alcohol concentrations, cleared in xylene and coverslipped in DPX mounting medium.

For fluorescent immunohistochemistry, free-floating slides were treated with 0.1 M glycine for 5 min in PBS 1 × and then with 1% SDS in PBS 1 × for 1 min at RT. Slides were blocked with 10% NGS, 1% BSA in PBS 1 × for 1 h at RT. The antibodies were diluted in 1% BSA, 0.3% Triton X-100 in PBS 1 ×. For double immunoflurescence, incubation with primary antibodies was performed overnight at RT and incubation with 1:500 Alexa fluor-conjugated secondary antibodies (Life Technologie) was performed for 2 h at RT. Nuclei were labelled with 1 µg/ml DAPI. For triple immunofluorescence, incubation with primary antibodies was performed overnight at RT, incubation with 1:500 Alexa fluor-conjugated secondary antibodies (Life Technologies) and 1:100 biotin-labelled secondary antibody (Sigma-Aldrich) was performed for 2 h at RT, followed by 1 h incubation in 1:100 streptavidin, Marina Blue conjugate (Life Technologies). Slides were mounted with mounting medium for fluorescence Vectashield (Vector Laboratories). The following primary antibodies were used: anti-TH 1:1000 (Sigma-Aldrich or Millipore), anti-FLAG 1:100 (Sigma-Aldrich), anti-MYC 1:100 (Cell Signaling) and anti-Hemoglobin 1:1000 (MP Biomedicals). For detection, Alexa fluor-488 or -594 (Life Technologies) were used. All images were collected using confocal microscopes (LEICA TCS SP2).

Quantification of DA neurons in the SNPc

The number of TH positive cells were determined by counting every fourth 40-µm sections as previously described (28). The delimitation between the ventral tegmental area and the SN was determined by using the medial terminal nucleus of the accessory optic tract as a landmark. All counts were performed blind to the experimental status of the animals through ImageJ software. TH+ cells were counted using “3D object counter tool”. Each found object has been quantified applying default settings. The following parameters were modified: Size filter set to 10-20 voxels, threshold set to: 128. Values were expressed as absolute quantification of unilateral SNpc TH+ cells.

Statistical Analysis

All data were obtained by at least three independent experiments. Data represent the mean ± S.E.M. and each group was compared individually with the reference control group using GraphPad Prism (v9) software. To compare the means of two samples, groups were first tested for normality, and then for homogeneity of variance (homoscedasticity). If the normality assumption was not met, data were analysed by nonparametric Mann-Whitney test. If the normality assumption was met, but homogeneity of variance was not, data were analysed by unpaired two-tailed t-test followed by Welch’s correction. If both assumptions were met, data were analysed by unpaired two-tailed t-test. To compare more than 2 groups One-Way ANOVA was used. Regarding statistical analysis of static rods experiments, each group were analysed by Chi-squared test. Significance to reference samples are shown as *, $p \leq 0.05$; **, $p \leq 0.01$; ***, $p \leq 0.001$; ****, $p \leq 0.0001$.

RESULTS

Biochemical analysis and structural characterization of α-syn PFFs preparation

Recombinant human α-syn fibrillation was monitored by thioflavin T (ThT) fluorescence and preformed fibrils (PFFs) were collected at plateau as long fibrils. Atomic force microscopy (AFM) was performed as previously reported (29) to confirm the presence of PFFs (Supplementary Figure 1a and b). Immunoblotting confirmed the presence of high molecular weight species in α-syn PFFs preparations by using

two epitope-specific antibodies, namely α-syn C-20 and α-syn SYN-1. The former is raised against the α-syn C-terminal epitope, recognising specifically FL-α-syn; the latter instead is specific for the α-syn C-terminal truncated species being immunoreactive to peptides containing 15 to 123 amino acid (Supplementary Figure 1c).

Both Ms and PFFs preparations contains monomeric and dimeric α-syn. High molecular weight species are detected in PFFs preparation as a smear.

In addition, both preparations present ΔC-α-syn species (Supplementary Figure 1d).

Prior to the main experiment, PFFs cellular internalization and the presence of pSer129 have been verified by immunofluorescence (IF) (Figure 1). Hb and control (CTRL) cells were supplemented with Alexa-488 labelled PFFs for 24 hours. As showed in Figure 1a small punctate structures were present inside the cells. PFFs uptake has been confirmed via a modified IF assay in which cells were incubated with Trypan blue that is reported to quench green fluorescence and to have affinity for amyloid fold (30). This assay confirmed the previous experiment (Supplementary Figure 1e).

Intracellular accumulation of α-syn was confirmed by western blot (Figure 1b) having both untreated and Ms-treated cells as negative controls. Moreover, α-syn PFFs inclusions were positively stained by the antibody recognizing pSer129 (Figure 1c), resembling one of the most prominent PTMs involved in α-syn fibrillation (8, 31).

Finally, the *in vitro* cytotoxicity of PFFs in both Hb and CTRL cells has been evaluated using methyl tetrazolium (MTT) assay at different time points. PFFs uptake induce a significant decrease of viable cells already after 24 hours treatment (Supplementary Figure 2).

Hb triggers the accumulation of a C-terminal truncated form of α-syn *in vitro*

To investigate the role of Hb in α-syn truncation we took advantage of DA iMN9D cell line stably overexpressing α and β-chains of Hb (Hb cells) forming the $\alpha_2\beta_2$ tetramer (17, 18, 32). We induced the prion-like conformational templating, mimicking the α-syn misfolding cyclic amplification, by supplying Hb and CTRL cells with pSer129 PPFs.

To characterize α-syn species in our model, we took advantage of epitope-specific antibodies for semi-quantitative western blot (WB) by using SYN-1 antibody in

comparison with SYN-C-20 (Supplementary Figure 1c).

Hb and CTRL cells were treated with PFFs for 24, 48 and 96 hours. Upon its administration, we analysed α-syn species at the different time points. Broadly, the expression of FL-α-syn decreased over time, whereas ΔC-α-syn species increased (Figure 2a and b), similarly to findings reported by Sacino and colleagues in neuronal-glial cultures and CHO cells (33). Extracellular α-syn species, instead, were stable over time (Supplementary Figure 3). Notably, ΔC-α-syn was reproducibly more abundant in Hb than CTRL cells at each time point and the levels of ΔC-α-syn normalized to FL-α-syn (ΔC-α-syn/FL-α-syn ratio) were higher in Hb than CTRL cells with a statistically significant difference at each time point (Figure 1a and c).

In the last decade, $nHb^{\alpha\text{-syn}}$ complexes have been identified in both non-human primates (NHP) and PD brains (19). Therefore, in order to assess Hb and α-syn PFFs interaction, iMN9D cell lysates were incubated with biotinylated PFFs and fibrils were pulled-down through NeutrAvidin resin. WB revealed that PFFs do not interact with Hb. Therefore, we concluded that ΔC-α-syn accumulation is not mediated by a direct protein interaction (Figure 2d and e).

Contribution of different proteases on the accumulation of α-syn C-terminal truncated species

The presence of ΔC-α-syn has been reported in the core of different types of aggregates in PD and Incidental Lewy Body Disease (34). C-terminal truncation of α-syn could be particularly detrimental as the ΔC-α-syn self-assembles into fibrils and increases the aggregation rate in both cultured cells (35, 36) and animal models (37-39). Both endogenous and pathologic α-syn undergo proteolytic processing producing truncations relevant for the disease. To date, the entirety of proteases forming truncated species found in human diseases have not been identified. However, proteases particularly prone to partial degradation of α-syn into ΔC-α-syn are already defined (40, 41) and include calpain I (Capn I), cathepsin D (Ctsd) and caspase 1 (Cas1) (12). Following the evaluation of the mRNA transcripts profile for Hb cells, we excluded caspase 1 from our study on the basis of its low expression (*data not shown*). To investigate the role of the Capn I in our *in vitro* model, we analysed the effect its specific inhibitor Capn inhibitor III (CI-III) on the ΔC-α-syn/FL-α-syn ratio.

iMN9D Hb cells were treated with vehicle DMSO (-) or CI-III (+) 24 hours prior amyloids administration. CI-III treatment was monitored at 24 and 48 hours. In both experimental conditions, treated cells presented increased levels of α-spectrin, a well-known Capn I substrate, in response to CI-III treatment (Figure 3e). ΔC-α-syn/FL-α-syn ratio decreased upon 48 hours of Capn I inhibition, proving this proteinase is involved in α-syn truncation in our experimental setting (Figure 3a and c).

To assess the role of Ctsd, Hb cells were treated with Pepstatin A, an inhibitor of acid proteases including Ctsd. In our model, 24 and 48 hours of treatment inhibited the protease activity approximately of 30% and 20%. However, a high mortality rate prevented an analysis on α-syn truncation (Supplementary Figure 4).

Hb overexpression in SNpc triggers the accumulation of ΔC-α-syn and loss of DA neurons

To study the effect of Hb in α-syn truncation and in dopamine neurons homeostasis *in vivo*, we injected a mixture of AAV9-2xFLAG-α-globin and AAV9-β-globin-MYC (indicated as AAV9-Hb) or with AAV9-CTRL bilaterally into the SNpc of mouse brain. We previously injected these AAV9-Hb in mice and we evaluated only the sub-acute effect of this treatment (17). The aim of this experiment was to monitor the animals for a longer time (9 months after the injection) for behavioural and biochemical alterations. Figure 4a shows the experimental protocol. Given the direct implication of Hb in both modulating α-syn truncation *in vitro* and impairing cognitive functions *in vivo* via DA depletion, we characterized the α-syn species of SNpc lysate of AAV9-CTRL and AAV9-Hb mice.

Mice overexpressing Hb presented an increased ΔC-α-syn/FL-α-syn ratio compared to control group (Figure 4b). These data proved that an aberrant expression of Hb increased the quantity of C-terminal truncated species, while FL-α-syn was unfazed as seen *in vitro* models. Importantly, Hb mice showed a decrease of tyrosine hydroxylase (TH) expression of about 50% (Figure 4c).

To understand whether the TH decrease seen in WB was due to a loss of neurons or to a decrease of TH enzyme expression, we performed immunohistochemistry analysis for TH in brain slices from AAV9-Hb or AAV9-CTRL mice and quantified A9 cells in in SNpc (Figure 4d). Results showed that Hb overexpression decreased DA

586 neurons in SNpc of about 50% (Figure 4e).

587 **Hb overexpression in SNpc decreases motor performances and trigger**
588 **cognitive impairments**

589 To determine whether AAV9-Hb induced behavioural alterations, we subjected mice
590 to a series of behavioural tests during the 9 months after the injection of the virus
591 (Figure 4a). We did not observe gross behavioural changes or abnormalities during
592 the assessment, with no difference in locomotor activity between the two groups at all
593 the time points examined (Figure 5a). Similarly, rotarod test did not show any motor
594 coordination impairment (Figure 5b). However, by using different assays for more fine
595 movement evaluation, we could observe a deficit in AAV9-Hb mice. In horizontal bars,
596 a test that measure the forelimb strength and coordination, AAV9-Hb mice were
597 performing worse than WT animals starting from 5 months after the injection (Figure
598 5c). Static rods test was used to evaluate the coordination of the mice to walk on
599 wooden rods of different diameter. In the wider rods (35, 25, 15 mm) there was not a
600 general worsening of the performance of AAV9-Hb mice, even if at some points AAV9-
601 Hb did performe worse (Supplementary Figure 5). In the 10 mm rods, that was the
602 narrowest one, mice often fall out of the rods both during orientation and transit and
603 AAV9-Hb mice failed to complete the test in a bigger proportion compared to AAV9-
604 CTRL, with the 9 months post-injection being the time with the widest difference
605 (Figure 5c and d). Since PD patients experience several non-motor symptoms such
606 as cognitive dysfunctions that often precede motor symptoms (42), we then tested
607 mice in two cognitive tests, the novel object recognition test (NOR) and the Y-maze
608 for spontaneous alternation, assessing recognition memory and spatial working
609 memory, respectively. In the NOR, AAV9-Hb mice showed a strong deficit in
610 recognizing the novel object, as indicating by the discrimination ratio (Figure 5e).
611 Moreover, in the Y-maze, AAV9-Hb mice displayed less spontaneous alternation
612 compared to AAV9-CTRL mice with no difference in the total entries in the arms
613 (Figure 5f). These data demonstrated that Hb expression in SNpc and the subsequent
614 partial loss of DA neurons induced mild motor impairments and cognitive deficits.

615 **DISCUSSION**

616 α-syn is a neuronal protein that is prone to misfold and polymerize into toxic fibrils.

These are the main component of LB, intracellular protein inclusions found in affected neurons in neurodegenerative diseases.

Although the triggering event is still unclear, gathering evidence prove the pivotal role of a particular PTM truncation of the carboxyl-terminal region of α-syn (ΔC-α-syn). ΔC-α-syn species are known to increase the pathological aggregation into LB inclusions both having a robust aggregation propensity itself and accelerating FL-α-syn aggregation. Indeed, increasing in prion-like seeding has been shown both *in vitro* and *in vivo* (11, 12, 43, 44). Gene expression profiling identified the transcript of α and β-chain of Hb in neurons, particularly enriched in A9 DA neurons (16, 45, 46). Several evidence correlate Hb in neurodegenerative diseases (47). An increased levels of Hb has been found in aging brain of rodents and humans as well as in neurons and glia of AD patients and in neurons of AD mouse models (45). In post-mortem brain from PD patients, α- and β-chains mRNAs levels were increased (48). Moreover, recent studies demonstrate that nHb may form complexes with α-syn in brain tissues of cynomolgus monkeys (19, 20). We previously demonstrated the association between Hb overexpression and the susceptibility to cell death of DA cell *in vitro* and that Hb overexpression caused nucleolar stress and autophagy inhibition (17). In this context, we focused on elucidating the potential interplay between Hb and α-syn.

To this purpose, we took advantage of iMN9D cells overexpressing α and β chains of Hb supplemented with PFFs known to recruit FL-α-syn to the core of the pathological inclusions and resemble LB features found in PD brains (49, 50). α-syn PFFs with pSer129 PTM were internalized by both Hb and CTRL cells. We demonstrated that FL-α-syn levels decreased over time and in treated Hb cells ΔC-α-syn was enriched by 3-fold as compared to control. The Hb-dependent ΔC-α-syn/FL-α-syn increased ratio suggests an Hb involvement in the α-syn C-terminal truncation mechanism.

Physiologic and pathologic production of C-terminal truncated species is mediated by different proteases, many of them directly correlating to the disease, as have been found co-localizing with ΔC-α-syn in LB inclusions (51). This is particularly the case for Capn I whose activity is found increased in the SNpc of PD patients (52). Interestingly, Capn I inhibitors ease pathologic features in mouse models of synucleinopathy (53). However, lysosomal cathepsins are known to be strongly involved in the normal breakdown of both monomeric and fibrillary α-syn (54). In this

framework, we investigated the role of Hb in the α-syn clearance and truncation by evaluating the ΔC-α-syn accumulation upon protease-specific inhibitors in Hb and CTRL cells. We identified Capn I as involved in C-terminal α-syn truncation since its selective inhibition reduced the ΔC-α-syn/FL-α-syn ratio. Conversely, insights on the role of CstD cannot be provided from this study since the inhibition of this protease was limited and caused massive cell death.

To characterize the involvement of Hb in α-syn C-terminal truncation, we induced Hb overexpression via bilateral AAV9-Hb injection in SNpc of mouse brain. Interestingly, ΔC-α-syn content in SNpc showed an increase of about 80% compared to AAV9-CTRL mice, recapitulating the effect obtained in the *in vitro* experiments. Although the increase is minor compared to the one observed *in vitro*, it is of note that we observed this enhancement on the endogenous α-syn levels, while *in vitro* cells were treated with PFFs. It would be interesting to study the role of Hb in animal models of synucleinopathies or in PD mouse models where α-syn is over-expressed (44). In the WB analysis we also noted a clear effect on TH levels in SNpc lysates indicating a potential loss of DA neurons. By counting DA cells in the SNpc we confirmed the partial loss (50%) of DA neurons in this area. Whether this loss is due solely to Hb over-expression or to the accumulation of the ΔC-α-syn species or to both of these phenomena has yet to be established. These data are consistent with the reduction of DA levels shown in animal models overexpressing ΔC-α-syn (55, 56). Along with neurodegeneration, such mice present deficits in locomotion and in cortical-hippocampal memory test (37). Moreover, passive immunization against ΔC-α-syn ameliorated neurodegeneration and neuroinflammation, reducing the accumulation of ΔC-α-syn and improved motor and memory deficits in a mouse model of PD (57). Yet, since the role of Hb in the degeneration of DA neurons is much less known, more studies are needed to unveil the precise role and the interplay between Hb and α-syn truncation *in vivo*.

As for several non-neurotoxin-based PD mouse model, the putative toxic effect on DA neurons of Hb over-expression was expected to be slow. Therefore, we monitored animals' behavior for 9 months after the virus injection. Consistent with the partial loss of DA neurons, we did not see overt motor impairments as indicated by locomotor activity and rotarod test. However, two tests that evaluate different motor skills showed

that AAV9-Hb mice displayed mild motor deficits. These results are in agreement with what observed in PD patients and animal models, where motor symptoms appear when most of the dopaminergic fibers are already lost (42). Before the onset of motor symptoms, PD patients often experience several non-motor deficits, such as cognitive impairments (42). Accordingly, a PD mouse model with bilateral partial 6-hydroxydopamine lesion showed a loss of about 60% of SNpc DA neurons, a mild motor phenotype (e.g. no locomotor activity alteration) and substantial cognitive deficits, as evidenced in NOR test and in other behavioural assays not related to motor functions (58). In this work, Hb mice have showed a similar loss of DA neurons, mild motor impairments and considerable cognitive deficits involving recognition and spatial working memory phenocopying features of the PD mouse model.

CONCLUSION

Our study indicates Hb a potential previously unrecognized modifier of PD that warrants further investigation. Several evidence demonstrates an increase of Hb expression in post-mortem brains of several neurodegenerative diseases including AD, PD and MSA. Given the effects of Hb overexpression in SNpc, an analysis of the correlation between genetic variation of Hb genes and nHb levels in the brain is needed to potentially associate nHb expression to the onset of neurodegenerative diseases, including PD.

ABBREVIATIONS

α-syn, alpha-synuclein;
Ms, monomers;
PTMs, post-translational modifications;
pSer-129, phosphorylated serine 129;
ΔC- α-syn, C-terminal truncated α-syn;
FL- α-syn, full-length α-syn;
PD, Parkinson’s disease;
LBD, Lewy Body Dementia;
MSA, Multiple System Atrophy;
SNpc, *Subtantia nigra pars compacta*;
GCIs, Glial cytoplasmic inclusions;

712 DA, dopaminergic;
713 Hb, hemoglobin;
714 nHb, neuronal Hb;
715 MPP^+, 1-methyl-4-phenylpyridinium;
716 PFFs, pre-formed fibrils;
717 AFM, Atomic force microscopy;
718 NHP , non-human primates;
719 Capn I, Calpain I;
720 Ctsd, cathepsin D;
721 Cas1, caspase 1;
722 TH, tyrosine hydroxylase;
723 NOR, novel object recognition;

724 **ACKNOWLEDGEMENTS**

725 We are indebted to all the members of the SG laboratory for thought-provoking
726 discussions. We are grateful to SISSA, IIT technical and administrative staff, especially
727 to Micaela Grandolfo, Omar Peruzzo and Eva Ferri, and Università del Piemonte
728 Orientale (UPO).

729 **FUNDING**

730 This work has been funded by intramural IIT support to SG and supported by the
731 Ministero dell'Università e della Ricerca (MIUR), Bando PRIN 2017-Prot.
732 2017SNRXH3 to FP.

733 **AVAILABILITY OF DATA AND MATERIALS**

734 The manuscript has data included as electronic Additional information.

735 **ETHICS APPROVAL**

736 All animal experiments were performed in accordance with European guidelines for
737 animal care and following Italian Board Health permissions (D.Lgs. 26/2014, 4 March
738 2014).

739 **COMPETING INTERESTS**

740 The authors declare no conflict of interest.

AUTHORS' CONTRIBUTIONS

CS designed, carried and analysed the *in vitro* experiments, wrote the manuscript; CB performed and analysed the *ex vivo* experiments, wrote the manuscript; ED carried out and analysed α-syn recombinant production and fibrillation; MC, ClS and FP analysed the data and discussed experimental results;
NJ, PP and PF discussed experimental results; PP performed and PF supervised AFM experiments; GL provide the fibrils, analysed the data and discussed experimental results; S.E. conceived the project and carried out the *in vivo* experiments, analysed the data and composed the manuscript; SG conceived the project, designed the experiments, supervised the study, and wrote the manuscript.
All authors contributed to this work, read the manuscript and agreed to its contents.

AUTHOR DETAILS

Affiliations:

[1]Area of Neuroscience, Scuola Internazionale Superiore di Studi Avanzati (SISSA), Trieste, Italy.
[2]Central RNA Laboratory, Istituto Italiano di Tecnologia (IIT), Genova, Italy.
[3]ELETTRA Synchrotron Light Source, Trieste, Italy.
[4]Department of Health Sciences and Research Center on Autoimmune and Allergic
[5]Diseases (CAAD), University of Piemonte Orientale (UPO), Novara, Italy.

Corresponding authors:

Correspondence to Stefano Gustincich or Stefano Espinoza.

REFERENCES

1. Bendor JT, Logan TP, Edwards RH. The function of alpha-synuclein. Neuron. 2013;79(6):1044-66.

2. Fusco G, De Simone A, Gopinath T, Vostrikov V, Vendruscolo M, Dobson CM, et al. Direct observation of the three regions in alpha-synuclein that determine its membrane-bound behaviour. Nat Commun. 2014;5:3827.

3. Fusco G, Pape T, Stephens AD, Mahou P, Costa AR, Kaminski CF, et al. Structural basis of synaptic vesicle assembly promoted by alpha-synuclein. Nat Commun. 2016;7:12563.

4. Serpell LC, Berriman J, Jakes R, Goedert M, Crowther RA. Fiber diffraction of synthetic alpha-synuclein filaments shows amyloid-like cross-beta conformation. Proceedings of the National Academy of Sciences of the United States of America. 2000;97(9):4897-902.

5. Aulić S, Le TTN, Moda F, Abounit S, Corvaglia S, Casalis L, et al. Defined $α$-synuclein prion-like molecular assemblies spreading in cell culture. BMC Neuroscience. 2014;15(1):69-.

6. Crowther RA, Jakes R, Spillantini MG, Goedert M. Synthetic filaments assembled from C-terminally truncated alpha-synuclein. FEBS Lett. 1998;436(3):309-12.

7. Iljina M, Garcia GA, Horrocks MH, Tosatto L, Choi ML, Ganzinger KA, et al. Kinetic model of the aggregation of alpha-synuclein provides insights into prion-like spreading. Proc Natl Acad Sci U S A. 2016;113(9):E1206-15.

8. Anderson JP, Walker DE, Goldstein JM, de Laat R, Banducci K, Caccavello RJ, et al. Phosphorylation of Ser-129 is the dominant pathological modification of alpha-synuclein in familial and sporadic Lewy body disease. J Biol Chem. 2006;281(40):29739-52.

9. Murray IVJ, Giasson BI, Quinn SM, Koppaka V, Axelsen PH, Ischiropoulos H, et al. Role of alpha-synuclein carboxy-terminus on fibril formation in vitro. Biochemistry. 2003;42(28):8530-40.

10. Hoyer W, Cherny D, Subramaniam V, Jovin TM. Impact of the acidic C-terminal region comprising amino acids 109-140 on alpha-synuclein aggregation in vitro. Biochemistry. 2004;43(51):16233-42.

11. Murray IV, Giasson BI, Quinn SM, Koppaka V, Axelsen PH, Ischiropoulos H, et al. Role of alpha-synuclein carboxy-terminus on fibril formation in vitro. Biochemistry. 2003;42(28):8530-40.

12. Sorrentino ZA, Giasson BI. The emerging role of alpha-synuclein truncation in aggregation and disease. J Biol Chem. 2020;295(30):10224-44.

13. Goedert M, Jakes R, Spillantini MG. The Synucleinopathies: Twenty Years On. Journal of Parkinson's disease. 2017;7(s1):S51-S69.

14. Liu CW, Giasson BI, Lewis KA, Lee VM, Demartino GN, Thomas PJ. A precipitating role for truncated alpha-synuclein and the proteasome in alpha-synuclein aggregation: implications for pathogenesis of Parkinson disease. J Biol Chem. 2005;280(24):22670-8.

15. Tu PH, Galvin JE, Baba M, Giasson B, Tomita T, Leight S, et al. Glial cytoplasmic inclusions in white matter oligodendrocytes of multiple system atrophy brains contain insoluble alpha-synuclein. Ann Neurol. 1998;44(3):415-22.

16. Biagioli M, Pinto M, Cesselli D, Zaninello M, Lazarevic D, Roncaglia P, et al. Unexpected expression of alpha- and beta-globin in mesencephalic dopaminergic neurons and glial cells. Proc Natl Acad Sci U S A. 2009;106(36):15454-9.

17. Codrich M, Bertuzzi M, Russo R, Francescatto M, Espinoza S, Zentilin L, et al. Neuronal hemoglobin affects dopaminergic cells' response to stress. Cell Death Dis. 2017;8(1):e2538.

18. Russo R, Zucchelli S, Codrich M, Marcuzzi F, Verde C, Gustincich S. Hemoglobin is present as a canonical alpha2beta2 tetramer in dopaminergic neurons. Biochim Biophys Acta. 2013;1834(9):1939-43.

19. Yang W, Li X, Li X, Li X, Yu S. Neuronal hemoglobin in mitochondria is reduced by forming a complex with alpha-synuclein in aging monkey brains. Oncotarget. 2016;7(7):7441-54.

20. Yang W, Li X, Li X, Yu S. Hemoglobin-alpha-synuclein complex exhibited age-dependent alterations in the human striatum and peripheral RBCs. Neurosci Lett. 2020;736:135274.

21. Zucca FA, Segura-Aguilar J, Ferrari E, Munoz P, Paris I, Sulzer D, et al. Interactions of iron, dopamine and neuromelanin pathways in brain aging and Parkinson's disease. Prog Neurobiol. 2017;155:96-119.

827 22. Ward PA, Till GO, Gannon DE, Varani JA, Johnson KJ. The role of iron in injury
828 of endothelial cells in vitro and in vivo. Basic Life Sci. 1988;49:969-74.
829 23. Rouault TA. Iron metabolism in the CNS: implications for neurodegenerative
830 diseases. Nat Rev Neurosci. 2013;14(8):551-64.
831 24. Biedler JL, Helson L, Spengler BA. Morphology and growth, tumorigenicity, and
832 cytogenetics of human neuroblastoma cells in continuous culture. Cancer research.
833 1973;33(11):2643-52.
834 25. Huang C, Ren G, Zhou H, Wang C-c. A new method for purification of
835 recombinant human alpha-synuclein in Escherichia coli. Protein expression and
836 purification. 2005;42(1):173-7.
837 26. Bousset L, Brundin P, Bockmann A, Meier B, Melki R. An Efficient Procedure
838 for Removal and Inactivation of Alpha-Synuclein Assemblies from Laboratory
839 Materials. Journal of Parkinson's disease. 2016;6(1):143-51.
840 27. Latawiec D, Herrera F, Bek A, Losasso V, Candotti M, Benetti F, et al.
841 Modulation of alpha-synuclein aggregation by dopamine analogs. PloS one.
842 2010;5(2):e9234-e.
843 28. Bensadoun JC, Deglon N, Tseng JL, Ridet JL, Zurn AD, Aebischer P. Lentiviral
844 vectors as a gene delivery system in the mouse midbrain: cellular and behavioral
845 improvements in a 6-OHDA model of Parkinson's disease using GDNF. Exp Neurol.
846 2000;164(1):15-24.
847 29. Aulić S, Masperone L, Narkiewicz J, Isopi E, Bistaffa E, Ambrosetti E, et al. α-
848 Synuclein Amyloids Hijack Prion Protein to Gain Cell Entry, Facilitate Cell-to-Cell
849 Spreading and Block Prion Replication. Scientific Reports. 2017;7(1):10050-.
850 30. Karpowicz RJ, Jr., Haney CM, Mihaila TS, Sandler RM, Petersson EJ, Lee
851 VMY. Selective imaging of internalized proteopathic alpha-synuclein seeds in primary
852 neurons reveals mechanistic insight into transmission of synucleinopathies. The
853 Journal of biological chemistry. 2017;292(32):13482-97.
854 31. Fujiwara H, Hasegawa M, Dohmae N, Kawashima A, Masliah E, Goldberg MS,
855 et al. alpha-Synuclein is phosphorylated in synucleinopathy lesions. Nature cell
856 biology. 2002;4(2):160-4.
857 32. Biagioli M, Pinto M, Cesselli D, Zaninello M, Lazarevic D, Roncaglia P, et al.
858 Unexpected expression of α- and β-globin in mesencephalic dopaminergic neurons

and glial cells. Proceedings of the National Academy of Sciences. 2009;106(36):15454 LP-9.

33. Sacino AN, Brooks MM, Chakrabarty P, Saha K, Khoshbouei H, Golde TE, et al. Proteolysis of alpha-synuclein fibrils in the lysosomal pathway limits induction of inclusion pathology. Journal of neurochemistry. 2017;140(4):662-78.

34. Prasad K, Beach TG, Hedreen J, Richfield EK. Critical role of truncated alpha-synuclein and aggregates in Parkinson's disease and incidental Lewy body disease. Brain pathology (Zurich, Switzerland). 2012;22(6):811-25.

35. Stefanova N, Klimaschewski L, Poewe W, Wenning GK, Reindl M. Glial cell death induced by overexpression of alpha-synuclein. J Neurosci Res. 2001;65(5):432-8.

36. Stefanova N, Seppi K, Scherfler C, Puschban Z, Wenning GK. Depression in alpha-synucleinopathies: prevalence, pathophysiology and treatment. J Neural Transm Suppl. 2000(60):335-43.

37. Hall K, Yang S, Sauchanka O, Spillantini MG, Anichtchik O. Behavioural deficits in transgenic mice expressing human truncated (1-120 amino acid) alpha-synuclein. Experimental neurology. 2015;264:8-13.

38. Tofaris GK, Goedert M, Spillantini MG. The Transcellular Propagation and Intracellular Trafficking of alpha-Synuclein. Cold Spring Harbor perspectives in medicine. 2017;7(9).

39. Periquet M, Fulga T, Myllykangas L, Schlossmacher MG, Feany MB. Aggregated alpha-synuclein mediates dopaminergic neurotoxicity in vivo. J Neurosci. 2007;27(12):3338-46.

40. Bassil F, Fernagut P-O, Bezard E, Pruvost A, Leste-Lasserre T, Hoang QQ, et al. Reducing C-terminal truncation mitigates synucleinopathy and neurodegeneration in a transgenic model of multiple system atrophy. Proceedings of the National Academy of Sciences of the United States of America. 2016;113(34):9593-8.

41. Wang W, Nguyen LTT, Burlak C, Chegini F, Guo F, Chataway T, et al. Caspase-1 causes truncation and aggregation of the Parkinson's disease-associated protein alpha-synuclein. Proceedings of the National Academy of Sciences of the United States of America. 2016;113(34):9587-92.

42. Kalia LV, Lang AE. Parkinson's disease. Lancet. 2015;386(9996):896-912.

43. Liu C-W, Giasson BI, Lewis KA, Lee VM, Demartino GN, Thomas PJ. A precipitating role for truncated alpha-synuclein and the proteasome in alpha-synuclein aggregation: implications for pathogenesis of Parkinson disease. The Journal of biological chemistry. 2005;280(24):22670-8.

44. Ulusoy A, Febbraro F, Jensen PH, Kirik D, Romero-Ramos M. Co-expression of C-terminal truncated alpha-synuclein enhances full-length alpha-synuclein-induced pathology. The European journal of neuroscience. 2010;32(3):409-22.

45. Richter F, Meurers BH, Zhu C, Medvedeva VP, Chesselet M-F. Neurons Express Hemoglobin α- and β-Chains in Rat and Human Brains. The Journal of comparative neurology. 2009;515(5):538-47.

46. Schelshorn DW, Schneider A, Kuschinsky W, Weber D, Krüger C, Dittgen T, et al. Expression of Hemoglobin in Rodent Neurons. Journal of Cerebral Blood Flow & Metabolism. 2008;29(3):585-95.

47. Freed J, Chakrabarti L. Defining a role for hemoglobin in Parkinson's disease. NPJ Parkinsons Dis. 2016;2:16021.

48. Ferrer I, Gomez A, Carmona M, Huesa G, Porta S, Riera-Codina M, et al. Neuronal hemoglobin is reduced in Alzheimer's disease, argyrophilic grain disease, Parkinson's disease, and dementia with Lewy bodies. J Alzheimers Dis. 2011;23(3):537-50.

49. Luk KC, Kehm V, Carroll J, Zhang B, O'Brien P, Trojanowski JQ, et al. Pathological alpha-synuclein transmission initiates Parkinson-like neurodegeneration in nontransgenic mice. Science (New York, NY). 2012;338(6109):949-53.

50. Luk KC, Kehm VM, Zhang B, O'Brien P, Trojanowski JQ, Lee VMY. Intracerebral inoculation of pathological alpha-synuclein initiates a rapidly progressive neurodegenerative alpha-synucleinopathy in mice. The Journal of experimental medicine. 2012;209(5):975-86.

51. Mishizen-Eberz AJ, Norris EH, Giasson BI, Hodara R, Ischiropoulos H, Lee VMY, et al. Cleavage of alpha-synuclein by calpain: potential role in degradation of fibrillized and nitrated species of alpha-synuclein. Biochemistry. 2005;44(21):7818-29.

52. Crocker SJ, Smith PD, Jackson-Lewis V, Lamba WR, Hayley SP, Grimm E, et al. Inhibition of calpains prevents neuronal and behavioral deficits in an MPTP mouse model of Parkinson's disease. J Neurosci. 2003;23(10):4081-91.

923 53. Diepenbroek M, Casadei N, Esmer H, Saido TC, Takano J, Kahle PJ, et al.
924 Overexpression of the calpain-specific inhibitor calpastatin reduces human alpha-
925 Synuclein processing, aggregation and synaptic impairment in [A30P]alphaSyn
926 transgenic mice. Hum Mol Genet. 2014;23(15):3975-89.
927 54. Sevlever D, Jiang P, Yen S-HC. Cathepsin D is the main lysosomal enzyme
928 involved in the degradation of alpha-synuclein and generation of its carboxy-terminally
929 truncated species. Biochemistry. 2008;47(36):9678-87.
930 55. Daher JPL, Ying M, Banerjee R, McDonald RS, Hahn MD, Yang L, et al.
931 Conditional transgenic mice expressing C-terminally truncated human alpha-synuclein
932 (alphaSyn119) exhibit reduced striatal dopamine without loss of nigrostriatal pathway
933 dopaminergic neurons. Molecular neurodegeneration. 2009;4:34-.
934 56. Wakamatsu M, Ishii A, Iwata S, Sakagami J, Ukai Y, Ono M, et al. Selective
935 loss of nigral dopamine neurons induced by overexpression of truncated human alpha-
936 synuclein in mice. Neurobiology of aging. 2008;29(4):574-85.
937 57. Games D, Valera E, Spencer B, Rockenstein E, Mante M, Adame A, et al.
938 Reducing C-terminal-truncated alpha-synuclein by immunotherapy attenuates
939 neurodegeneration and propagation in Parkinson's disease-like models. The Journal
940 of neuroscience : the official journal of the Society for Neuroscience.
941 2014;34(28):9441-54.
942 58. Bonito-Oliva A, Pignatelli M, Spigolon G, Yoshitake T, Seiler S, Longo F, et al.
943 Cognitive impairment and dentate gyrus synaptic dysfunction in experimental
944 parkinsonism. Biol Psychiatry. 2014;75(9):701-10.
945

946 **FIGURES:**

Figure 1

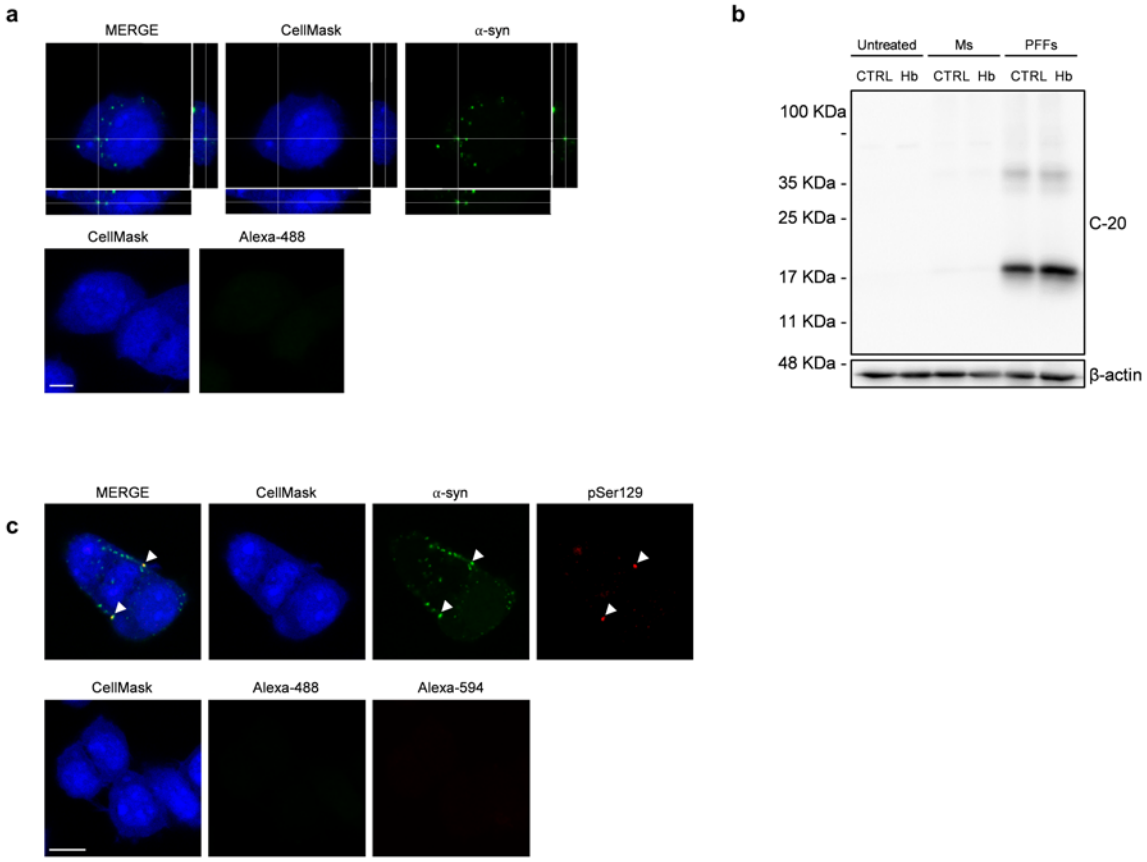

947

948 **Sonicated α-syn fibrils are internalized by iMN9D cells and are positively stained by pSer129**
949 **antibody.** Representative confocal microscopy images of Hb cells treated with Alexa-488 labelled PFFs
950 for 24 h. Cells not incubated with labelled PFFs were used to establish autofluorescence levels. Entire
951 cells were labelled by CellMask (**a**). Immunoblot of lysates from untreated cells and cells treated with
952 Ms and PFFs for 24 h (**b**). Representative confocal microscopy images of CTRL and Hb cells
953 immunostained for α-syn phosphorylated at Ser129 (pSer129, Alexa 594, red). Arrows indicate
954 intracellular inclusions positive to pSer129 antibody. Cells incubated only with secondary antibody were
955 used to establish autofluorescence levels. Nuclei were stained with DAPI. Scale bar 10 μm (**b**).

956

Figure 2

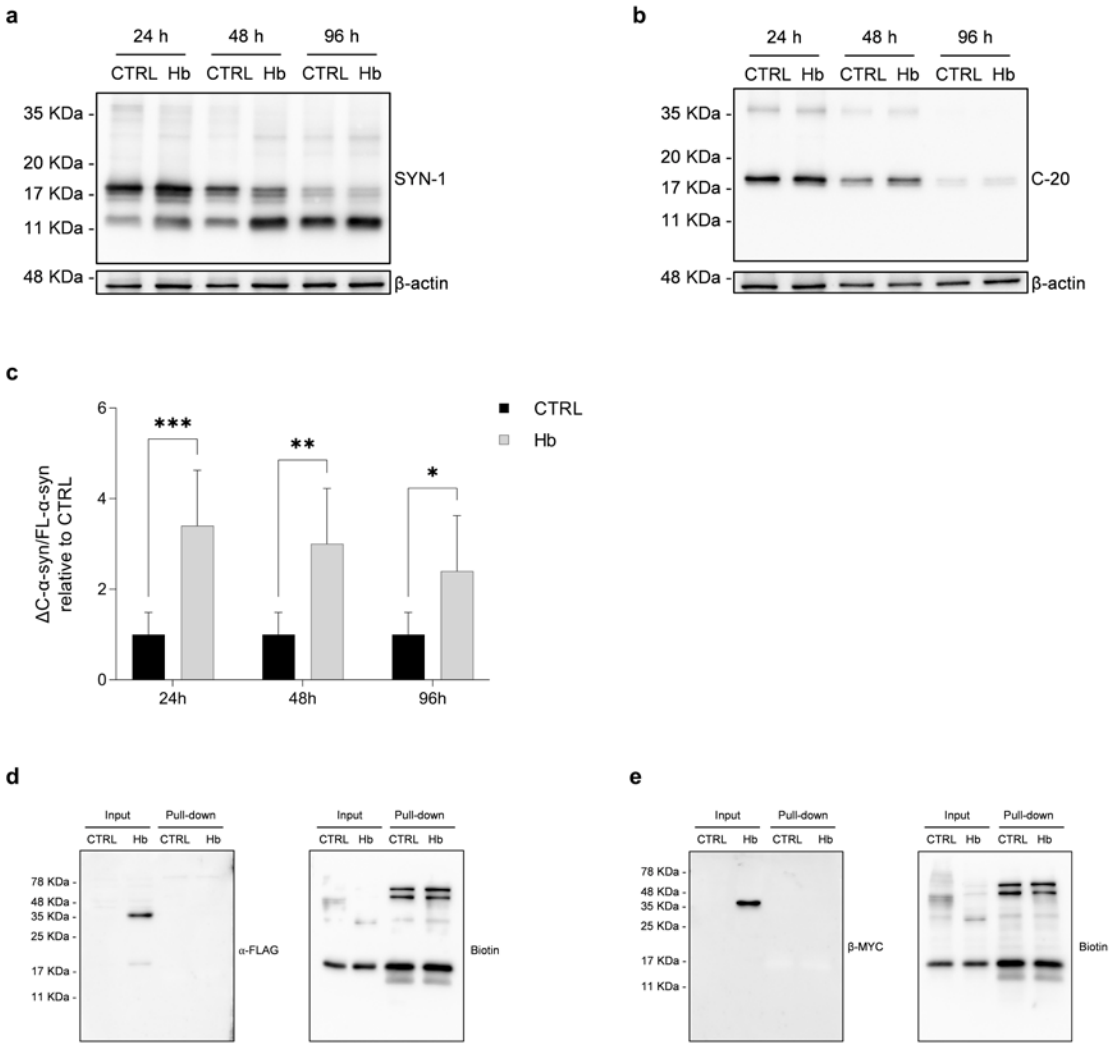

C-terminal truncated α-syn accumulation in the presence of Hb in cell lysates. CTRL and Hb cells were treated with α-syn amyloids. Cell lysates were collected at the indicated time points. Cell lysates were analysed by immunoblotting with SYN-1 (**a)** and C-20 antibodies (**b**). Band intensity corresponding to ΔC-α-syn and FL-α-syn was quantified and the ratio was calculated. Data represent means ± SEM and are representative of six independent experiments. Statistical analysis was performed with one-way Anova. *, p ≤ 0.05; **, p ≤ 0.01; ***, p≤ 0.001; ****, p ≤ 0.0001; ns, not significant (**c**). Pull down of biotinylated PFFs in iMN9D cell lysates from both CTRL and Hb cells were revealed by immunoblot with anti-FLAG (**d**) and anti MYC (**e**) antibodies. Samples were also revealed with anti-biotin antibody as control of the experiment.

Figure 3

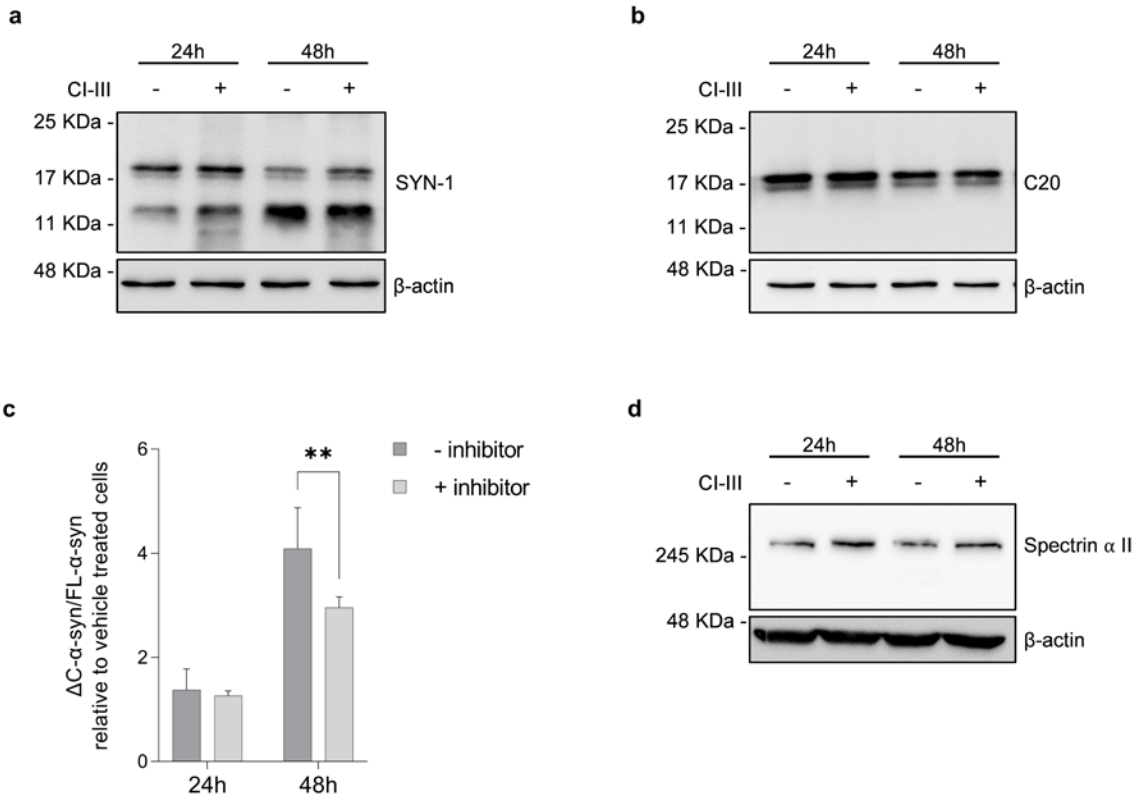

968

969 **Effect of Calpains inhibition on α-syn C-terminal truncated species accumulation in Hb cells.**
970 Cell lysates of Hb cells treated with DMSO (-) and Calpain inhibitor III (+) were analysed by
971 immunoblotting with SYN-1 (**a**) and C-20 (**b**) antibodies. Band intensity corresponding to ΔC-α-syn and
972 FL-α-syn was quantified and the ratio was calculated. Data represent means ± SEM and are
973 representative of six independent experiments. Statistical analysis was performed with one-way Anova.
974 *, $p \leq 0.05$; **, $p \leq 0.01$; ***, $p \leq 0.001$; ****, $p \leq 0.0001$; ns, not significant (**c**). Cell lysates of Hb cells
975 treated with DMSO (-) and CI-III (+) were analysed by immunoblotting with anti-Spectrin α II antibody
976 (**d**).

977

Figure 4

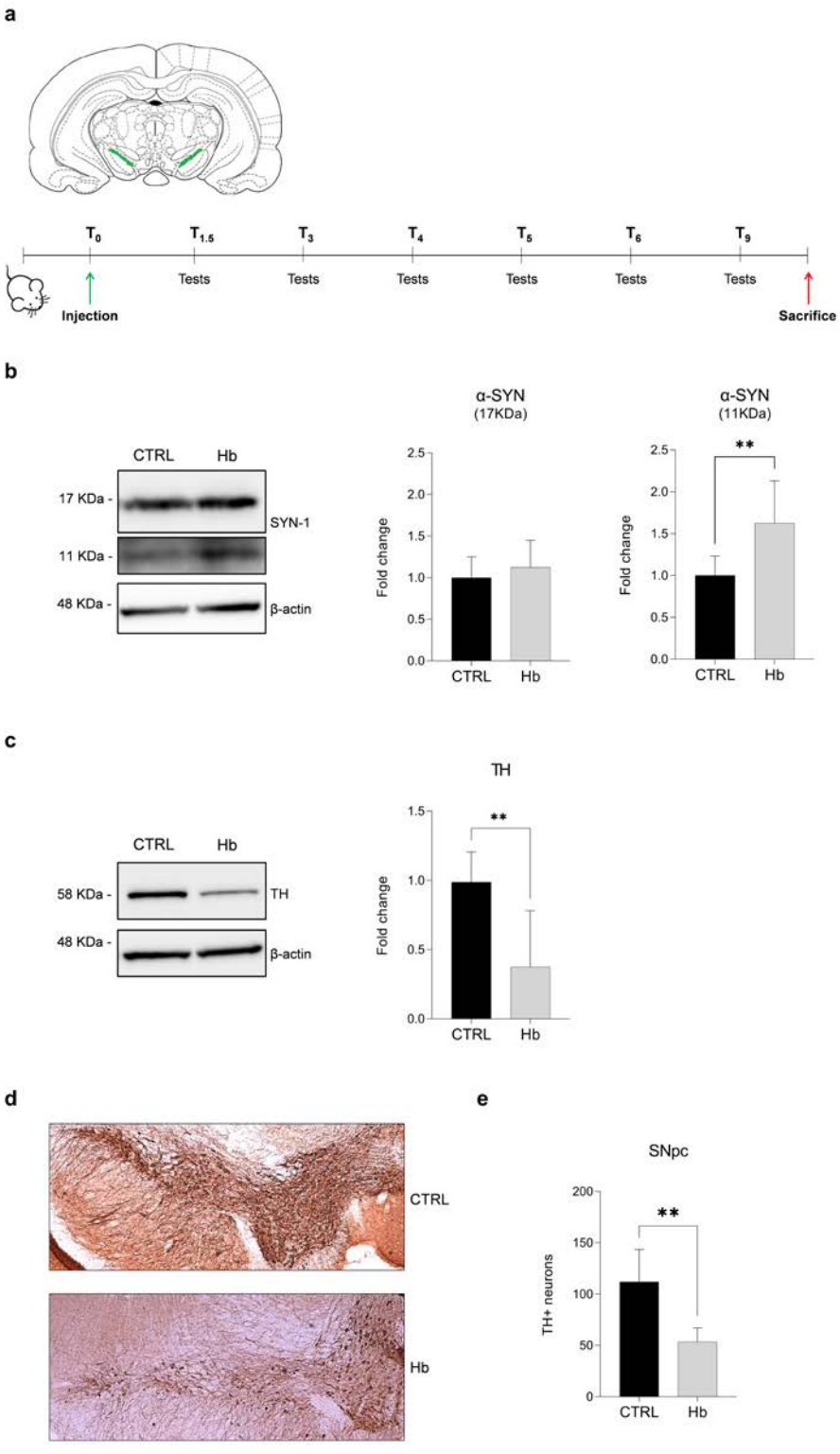

Hb overexpression in SNpc triggers the accumulation of ΔC-α-syn and loss of DA neurons. Scheme representing the experimental protocol used for the assessment Hb overexpression. AAV9 expressing Hb (AAV9-Hb) and AVV9-CTRL were bilaterally injected in the brain of 3-months old mice.

Brain diagram indicating SNpc (green) as the region of the injection (*upper panel*). Behavioral tests were performed to verify the locomotor performance of mice 1.5, 3, 4, 5, 6 and 9 months post-injection (*lower panel*) (**a**). Level of expression in SNpc of Hb and CTRL mice (n=4) at 10 months post-injection of FL-α-syn (17 KDa), ΔC-α-syn (11 KDa) (**b**, *left panel*) and tyrosine hydroxylase (TH, 58 KDa) (**c**, *left panel*) was assessed by western blot. Band intensity was quantified (**b** and **c**, *right panel*). TH-positive neurons of the SNpc were evaluated by immunohistochemistry (**d**, *left panel*) and quantified (**d**, *right panel*) for Hb and CTRL mice (n=4; 3 slices each). Data represent means ± SEM. Statistical analysis was performed with unpaired t test with Welch's correction. *, $p \leq 0.05$; **, $p \leq 0.01$; ***, $p \leq 0.001$; ****, $p \leq 0.0001$; ns, not significant.

Figure 5

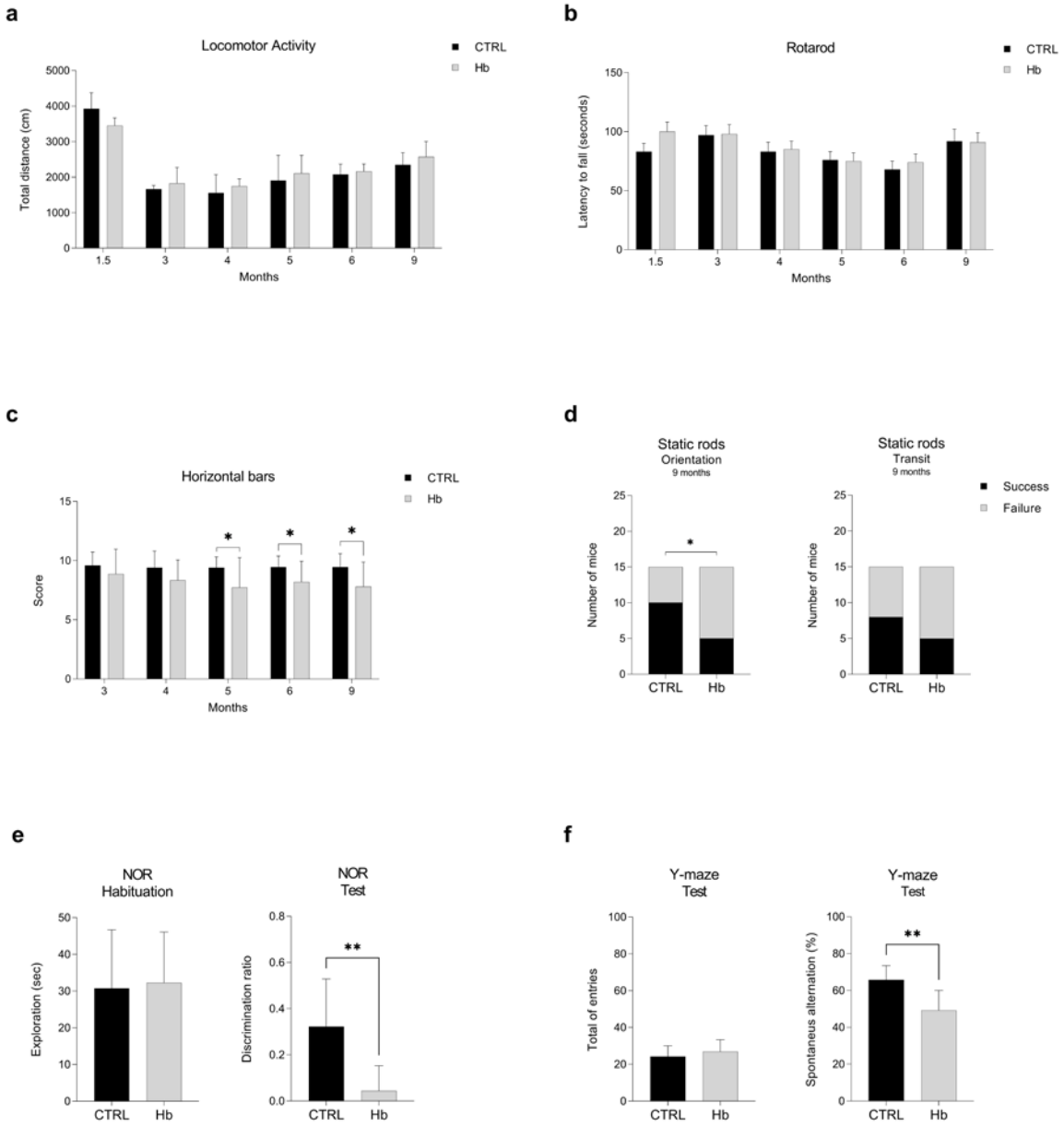

Hb overexpression in SNpc decrease motor performances and trigger cognitive impairments. AAV9-CTRL (n=12) and AAV9-Hb (n=12) were assessed for locomotor activity and total distance (cm) was recorded at different time points after injections (**a**). AAV9-CTRL (n=15) and AAV9-Hb (n=15) were also scored for motor coordination with the rotarod test (**b**) and latency to fall was measured. Horizontal bars test as used to assess forelimb strength and coordination (**c**) and mice were scored for their performance. AAV9-CTRL (n=15) and AAV9-Hb (n=15). Data represent means ± SEM. Statistical analysis was performed with unpaired t test with Welch's correction. *, $p \leq 0.05$. AAV9-CTRL (n=15) and AAV9-Hb (n=15) were assessed in static rods test measuring two parameters, transit time and orientation time (seconds) and different time points. In panel (**d**) it is depicted the results at 9 months

after injection. Chi-square test was used to evaluate the success/failure of each group. *, $p \leq 0.05$. Novel object recognition test (NOR) was used to evaluate recognition memory (**e**). AAV9-CTRL (n=8) and AAV9-Hb (n=8) was habituated to the object for 10 minutes and exploration (seconds) of the objects was measured (**e**, *left panel*). After 1 hours, mice were assessed to recognize the novel object and the discrimination ration was plotted (**e**, *right panel*). Spontaneous alternation in the Y-maze was used to measured spatial working memory in AAV9-CTRL (n=10) and AAV9-Hb (n=12) mice (**f**). Total entries were calculated for each group (**f**, *left panel*). Spontaneous alternation % was plotted for each group (**f**, *right panel*). Data represent means ± SEM. Statistical analysis was performed with unpaired t test with Welch's correction. *, $p \leq 0.05$; **, $p \leq 0.01$.